Available online at www.sciencedirect.com
ScienceDirect
Journal of the European Ceramic Society 28 (2008) 2399–2404
www.elsevier.com/locate/jeurceramsoc

Crystallization behavior of the eutectic glass in the C12A7–$CaYAlO_4$ system

Naonori Sakamoto *, Kazunari Suda, Tomoaki Watanabe, Nobuhiro Matsushita, Masahiro Yoshimura

Materials and Structures Laboratory, Tokyo Institute of Technology, 4259 Natastuta, Midori-ku, Yokohama 226-8503, Japan

Available online 4 March 2008

Abstract

Crystallization behavior during annealing of eutectic glass in the C12A7–$CaYAlO_4$ system was investigated by SEM, STEM, XRD, and TG–DTA. At 900 °C, phase separation of Y-poor and Y-rich phases appeared without crystallization. The phase separation might lead bulk crystallization of C12A7 by subsequent crystallization. At 950 °C, crystallization of unknown metastable phase was observed together with C12A7 crystallization. Above 1000 °C, crystallization of $CaYAlO_4$ and C12A7 was observed. Crystallization behavior was schematically explained and bulk crystallization of C12A7 was explained by the phase separation.

Keywords: Composites; Al_2O_3; Glass; Glass ceramics; Eutectic

1. Introduction

Calcium aluminate glasses have been of great interest due to their high transparency of IR region, ~5 μm, which cannot be obtained by the conventional glass systems based on silica networks.[1] Despite the advantage, calcium aluminate glass is not widely used as a glass material by itself because it is difficult to fabricate them without crystallization; it is readily devitrified during cooling. To our knowledge, inviscid melt spinning is the only technique to fabricate calcium aluminate glass fibers without mixing any other components.[2,3] The other ways to fabricate the calcium aluminate-based glass is mixing SiO_2, BaO, SrO, etc. into the calcium aluminate glass to obtain higher glass formability than pure $CaO–Al_2O_3$ glasses. Recently, we have reported a fabrication technique for a bulk of calcium aluminate-based glass in the eutectic $Y_2O_3–CaO–Al_2O_3$ system,[4] where the glass phase were easily obtained by conventional molding technique and the glass showed high transparency up to ~5 μm. Our research has been based on a ternary eutectic system rather than a binary eutectic. An advantage to using the ternary eutectic is its low melting point and a high glass formability which enables to fabricate bulk ceramics from melt. In the ternary eutectic system of $HfO_2–Al_2O_3–GdAlO_3$, we have also successfully fabricated an amorphous phase.[5,6]

The calcium aluminate crystal, especially $12CaO·7Al_2O_3$ (C12A7), is also recently of great interest. C12A7 has been known as one component of alumina cement, but it has gathered attention due to several remarkable properties, i.e. O^-, O^{2-}, and H^- emission and clathration of electrons at room temperature (so-called electride materials).[7–9] Kim et al.[10] improved fabrication techniques for the C12A7 material and showed possibilities of a new route by melting in strong reduction atmosphere.[10] We have reported a fabrication route for the C12A7-based bulk composites using the ternary eutectic $Y_2O_3–CaO–Al_2O_3$ system, where the C12A7 bulk composite can be easily obtained by merely annealing the molded glass.[11] The shape and size of the composite can be controlled by the glass because it does not cause any cracking during annealing, although the C12A7 stoichiometry glass cracks during annealing. In that report, we suggested a mechanism of cracking and of avoiding cracking. However, our explanation was not based on enough data such as cross-sectional observation of samples annealed at several temperatures.

In the present paper, we focus on the precise crystallization behavior in order to understand crystallization behavior of the $Y_2O_3–CaO–Al_2O_3$ system. The crystallization behavior of the

* Corresponding author.
E-mail address: tnsakam@ipc.shizuoka.ac.jp (N. Sakamoto).

0955-2219/$ – see front matter © 2008 Elsevier Ltd. All rights reserved.
doi:10.1016/j.jeurceramsoc.2008.01.010

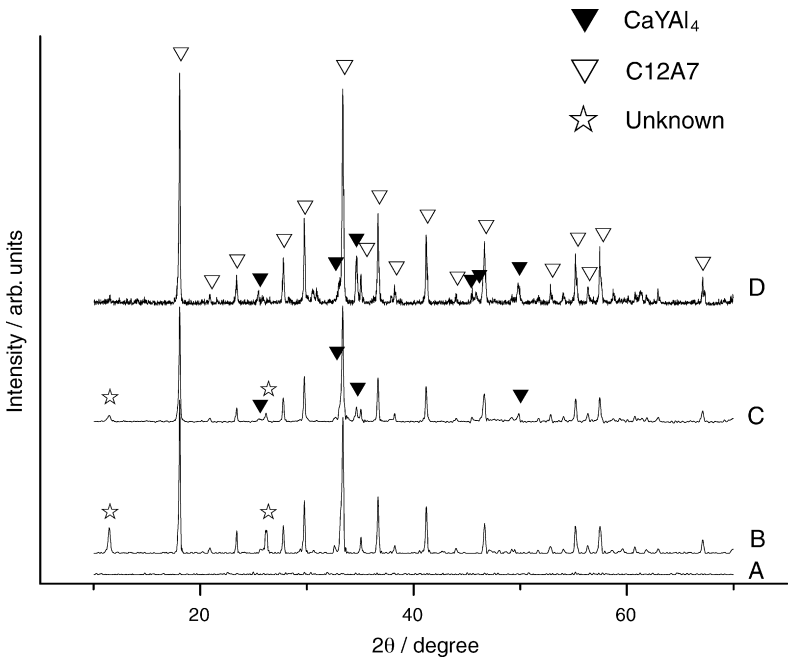

Fig. 1. XRD patterns for the sample A (900 °C–6 h annealing), B (950 °C–6 h annealing), C (1000 °C–6 h annealing), and D (1200 °C–6 h annealing). No particular crystalline peaks appeared in the sample A. The sample B was composed of C12A7 and unknown phase. The sample C was composed of the three phases, C12A7, the unknown phase, and $CaYAlO_4$. The sample D included only two phases of C12A7 and $CaYAlO_4$. The unknown phase peaks decreased with increasing annealing temperature, whereas contrarily, $CaYAlO_4$ peaks increased with increasing annealing temperature.

ternary system can also be meaningful to those who are interested in the other calcium aluminate-based glasses because there are few reports related to crystallization behavior of the calcium aluminate glasses except for ordinary calcium aluminate compositions.[12–15]

2. Experimental

A eutectic composition between C12A7 and $CaYAlO_4$ pseudo-binary system (Y_2O_3:CaO:Al_2O_3 = 2.50:61.92:35.58 mol%) were selected to investigate the crystallization behavior. Mixed sample powder of Y_2O_3 (99.999%, Shin-Etsu Chemical Co. Ltd., Tokyo, Japan), $CaCO_3$ (99.5%, Cica-Reagent, Kanto Chemical Co. Inc., Tokyo, Japan) and Al_2O_3 (99.99%, AKP-30, Sumitomo Chemical Co. Ltd., Tokyo, Japan) for the eutectic composition was uniformly blended using an alumina mortar with adding ethanol. After drying at 80 °C for 1 h in an electric oven under normal air, the mixture was melted and solidified using an arc-imaging furnace. Detailed procedures for the arc-image furnace (UF-10001, Ushio Inc., Tokyo, Japan) are mentioned in our previous papers.[4,5,11,16] The sample after the solidification had globule shape due to the surface tension of the melt and vitrified caused by rapid cooling rate about 200–500 °C/s. The sample globules were annealed at several temperatures and several time periods, i.e. 900 °C–6 h (stated as sample A), 950 °C–6 h (sample B), 1000 °C–6 h (sample C) and 1200 °C–6 h (sample D).

Samples after annealing were ground using alumina mortar for X-ray diffraction (XRD) (Cu Kα, MXP3VA, Bruker AXS K.K., Kanagawa, Japan). The globule sample without grinding was subjected to thermogravimetry and differential thermal analysis (TG–DTA) (Type 2020, Bruker AXS K.K., Kanagawa, Japan) in order to ignore the mechanical stress or increased surface effects by grinding. Sample morphologies were observed by scanning electron microscopy (SEM) (S4500, Hitachi High-Technologies Corporation, Tokyo, Japan) and scanning transmission electron microscopy (STEM) (JEM-3100FEF, JEOL Ltd., Tokyo, Japan). The backscattered electrons were used for the SEM imaging for the sample A, C, and D, whereas the secondary electrons were used for the sample B. Elemental analyses were examined by energy dispersive X-ray fluorescence spectrometer (EDS) attached with SEM and STEM. SEM samples for cross-sectional observation were prepared by mechanical polishing, whereas the STEM sample was prepared by mechanical polishing and subsequent Ar gas milling (EM-09100IS Ion Slicer, JEOL Ltd., Tokyo, Japan).

3. Results and discussion

Fig. 1 shows XRD patterns of the samples after annealing at several temperatures. Sample A, annealed at 900 °C, showed no crystalline peak, whereas the three samples B–D, which were annealed above 950 °C, showed crystal phases. Sample B showed C12A7 and unknown crystalline peaks at 11.47° and 26.21° (corresponding *d*-values were 0.771 nm, and 0.340 nm, respectively). Sample C consisted of C12A7, the unknown crystalline, and $CaYAlO_4$. Sample D consisted of only the end members of the eutectic system, C12A7 and $CaYAlO_4$. The unknown crystalline can be considered as a metastable phase because the unknown peaks decreased with increasing annealing temperature. The unknown phase might be also complementary to the $CaYAlO_4$ phase since the unknown peaks conversely

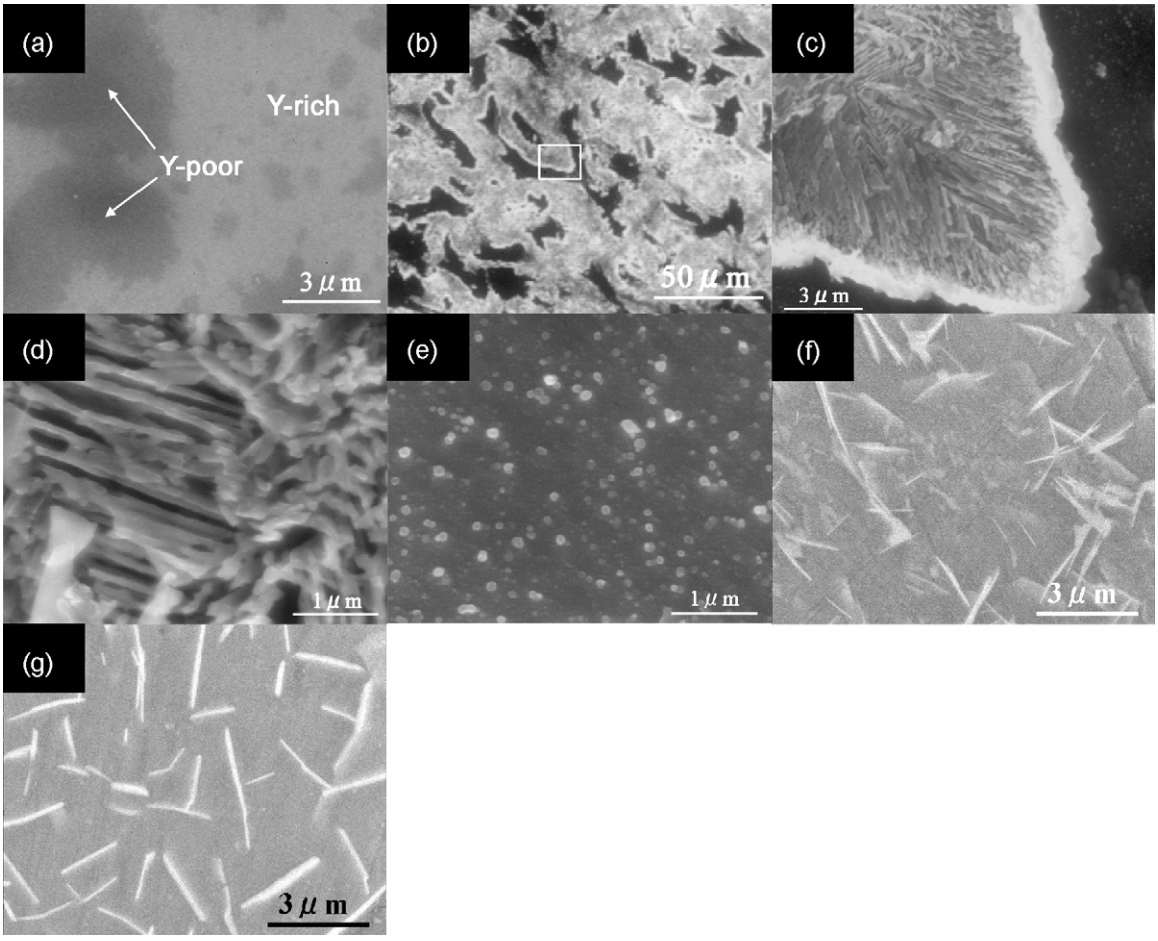

Fig. 2. SEM cross-sectional images of the samples A(a), B(b–e), C(f), and D(g). Rectangle frame inserted to the image (b) indicates the observing area of the image (c). Images (d) and (e) are enlarged views of bundles and granules in the sample B. The sample A showed phase separation into Y-poor and Y-rich phases. The sample B was composed of two phases with different morphologies, bundles and granules. The samples C and D were composed of matrix and plate shape particles.

decreased with increasing annealing temperature. Therefore, one can recognize that the unknown phase is composed of Y as well as Ca, Al and O.

Fig. 2 shows cross-sectional SEM images of the samples after annealing. The sample A was composed of two phases of dark and light as shown in Fig. 2(a), where the dark phases had non-uniform shapes of approximately hundreds of nanometer to 10 μm in size. Generally in the SEM backscattered image, the brightness of components should reflect the atomic number rather than the surface morphology,[14] i.e. particles consisted of heavy elements looks brighter than that of light elements. Therefore, the dark and light phases in Fig. 2(a) imply that they are Y-poor and Y-rich phases, respectively. As shown in Fig. 1, the sample A includes no crystal phases, therefore, the two phases in the SEM image can be considered amorphous phases of Y-poor and Y-rich. The sample B was composed of two phases, bundles of 3–5 μm in length and granules of several tens to one hundred nm in diameter, as shown in Fig. 2(b)–(e). EDS obtained from the bundle and the granules were shown in Fig. 3(a) and (b), respectively. Both of the EDS peaks showed Ca, Al, Y, and O, and no particular impurity was included. Although Y was overlapping an escape peak of Ca, which was caused by Si element composed of a window of EDS detector, EDS from the bundle showed significantly high intensity of Y element compared to that from the granules. By considering a result from XRD and SEM, it can be recognized that the bundles containing Y are the unknown crystalline and the granules are C12A7.

As shown in Fig. 2(b) and (c), the sample B showed a ragged cross-sectional surface even after mechanical polishing by the same method as the other samples, and the granules area seemed to be ground much more than the bundle area. This might be caused by a significantly different mechanical strength between these two phases against polishing/grinding, i.e. the bundles are much stronger than the granules. Samples C and D showed two phases of plate and matrix as shown in Fig. 2(f) and (g). The plate was approximately 1–3 μm in length and isolated. In the same logic as the sample A, the plates and the matrix can be considered as $CaYAlO_4$ and C12A7, respectively. The $CaYAlO_4$ grains of sample D were thicker than the sample C due to high crystal growth rate caused by high temperature annealing. Fig. 4(a) shows STEM image of the sample D. The microstructure observed by STEM was a reverse of SEM image, where the $CaYAlO_4$ plates looked dark compared to the C12A7 matrix. STEM–EDS mapping by Y(L) characteristic X-ray elementally confirmed these phases as shown in Fig. 4(b). Most

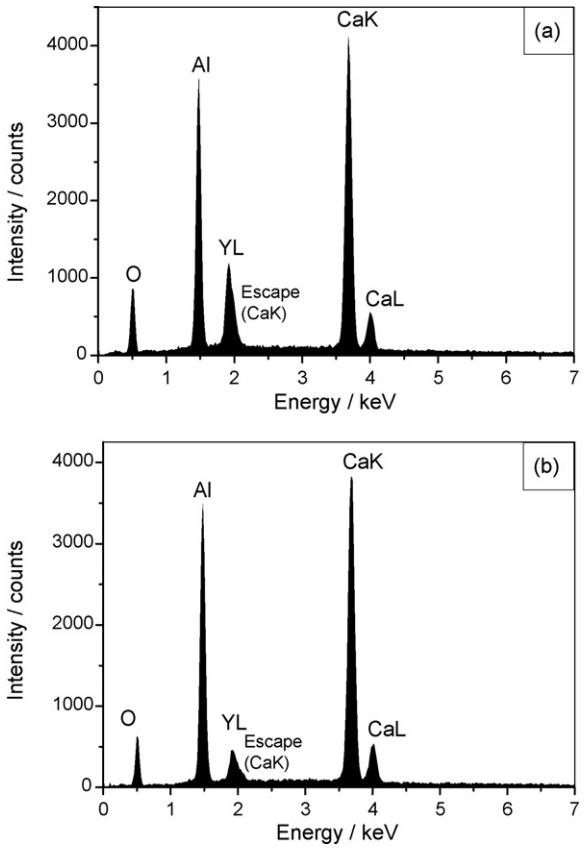

Fig. 3. EDS peaks obtained from the bundle (a) and from the granules (b) of the sample B. The bundle showed higher Y(L) peak than the granules, therefore, the bundle can be considered as Y-rich phase, i.e. the unknown phase.

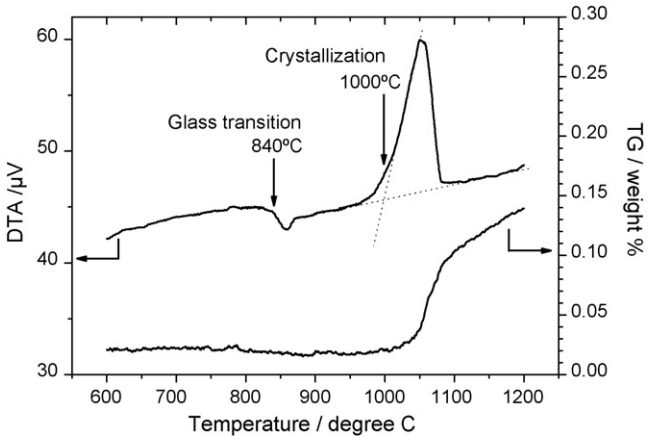

Fig. 5. TG–DTA of the globule glass sample. DTA curve showed a glass transition and a crystallization peak appeared at 840 °C and 1000 °C, respectively. Weight increase indicated a nature of C12A7 crystal, which shows water uptake at 1000 °C from air.

of the $CaYAlO_4$ phases were rod shape but some of them were plate shape of 1–3 μm in size, therefore, one can consider the $CaYAlO_4$ is plate shape rather than rod shape. The matrix phase did not show any particular peak of Y element in it, therefore, it can be considered as pure C12A7 matrix, which was confirmed by the high-resolution lattice image (not shown).

Fig. 5 shows TG–DTA profile for the globule glass sample. The glass transition temperature appeared approximately at 840 °C and an exothermic peak corresponds to crystallization appeared at approximately 1000 °C. The crystallization temperature was considerably high compared to our previous measurement,[4] 890 °C, where the sample was ground before measurement. It can be understood that reduced nucleation rate caused by smaller surface area of globule (∼3 mm in size) than that of the ground powder (>10 μm in size) raised its crystallization temperature. No peak corresponds to crystallization of the metastable phase was found at around 950 °C in the present DTA line obtained by globule sample, although the globule sample B was annealed at 950 °C in this study. This can be explained by annealing time periods. The crystallization of the metastable phase might not occur readily under a heating rate of 10 °C/min. but the crystallization of $CaYAlO_4$ occurs from the metastable phase or directly from glass. Then, the annealing at 1000 °C or 1200 °C under 10 °C/min heating rate crystallize $CaYAlO_4$ and C12A7 rather than the metastable phase, whereas holding below $CaYAlO_4$ crystallization temperature, approximately 1000 °C, e.g. 950 °C for 6 h, crystallize the metastable phase. TG curve showed continuous weight increase starts from approximately 1040 °C accompanied by the crystallization. The weight increase, which was also observed for the powder sample, can be recognized as a unique nature of the C12A7, water uptake from air.[17,18]

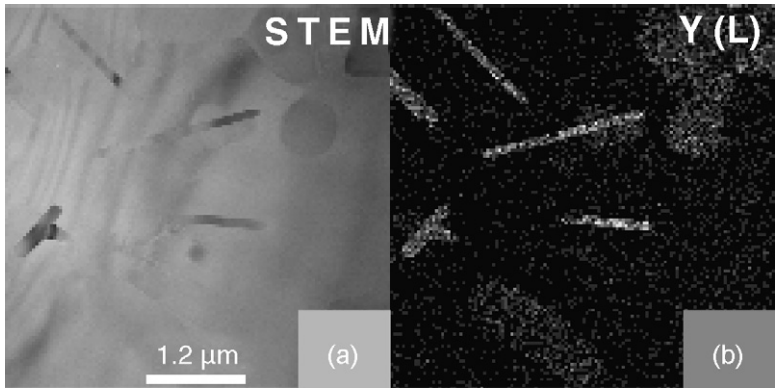

Fig. 4. STEM image of the sample D (a) and corresponding EDS mapping by Y(L) X-ray. The EDS mapping obviously indicated the plate particles were composed of Y elements, whereas the matrix was not composed of Y elements. It was confirmed that the plate particles and matrix were $CaYAlO_4$ and C12A7, respectively.

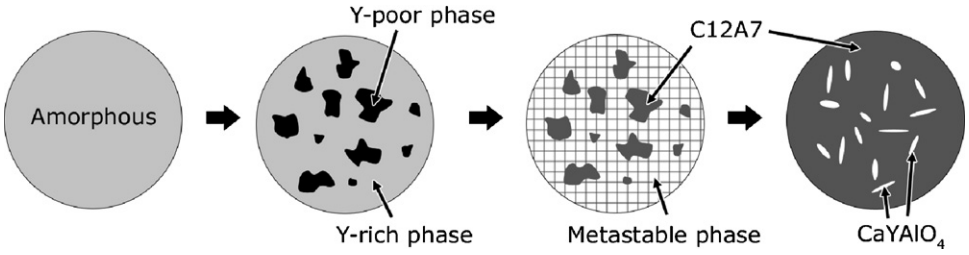

Fig. 6. Schematic representation of crystallization behavior of the C12A7–$CaYAlO_4$ eutectic glass. At the first stage of annealing, phase separation into Y-poor and Y-rich phases occurs without crystallization. At the second stage, the metastable phase crystallize from the Y-rich phase and the C12A7 crystallize from Y-poor phase. At the third stage, $CaYAlO_4$ and C12A7 phases are crystallized from the metastable phase.

Fig. 6 shows a schematic crystallization behavior of the sample at each time period during annealing. At the first stage of annealing, phase separation occurs into two phases of Y-poor and Y-rich without crystallization under a supercooled liquid state. At the second stage, the metastable phase starts to crystallize from the Y-rich phase and the C12A7 starts crystallize from Y-poor phase. The phase separation should encourage crystallization of these two phases because it increases a degree of supersaturation for each crystal phase in the supercooled liquid. At the third stage, the metastable phase are decomposed into $CaYAlO_4$ and C12A7. It should be indicated that the phase separation leads bulk crystallization of C12A7.

As reported in our previous paper,[11] glass of C12A7 stoichiometry composition cracks during annealing due to crystallization of C12A7, whereas the eutectic glass of C12A7–$CaYAlO_4$ system does not. We suggest the cracking mechanism by volume expansion of C12A7 during annealing[19] and surface crystallization nature of the stoichiometric glass.[20] We also suggested the cracking avoiding mechanism of the eutectic glass by complementary volume shrinkage of $CaYAlO_4$. However, as indicated in our present study, the bulk crystallization of the eutectic glass caused by the phase separation is to be one significant phenomenon which helps to avoid cracking as well as the other reasons stated in the previous paper. The crystallization behavior suggested here does not take into account of any time periods during annealing. Therefore, in the practical case with limited time, i.e. 10 °C/min. heating rate, the phase separation and the crystallization of metastable phase does not accomplish and does not give large size phases as written in Fig. 6. However, the phase separation will lead the bulk crystallization of C12A7 which leads to avoid cracking during annealing.

4. Conclusion

Crystallization behavior from C12A7–$CaYAlO_4$ eutectic glass was observed by SEM, TEM, XRD and TG–DTA. It was observed that phase separation of Y-poor and Y-rich amorphous phases (at 900 °C), crystallization of metastable phase and C12A7 from the separated amorphous (950 °C), and crystallization of $CaYAlO_4$ and C12A7 from the metastable phase (above 1000 °C). Crystallization behavior was schematically explained and bulk crystallization of C12A7 was explained by the phase separation.

Acknowledgments

A part of this work was supported by the "Nanotechnology Support Project" of the Ministry of Education, Culture, Sports, Science and Technology (MEXT), Japan. The authors are thankful to Drs. Y. Bando and M. Mitome in NIMS for analyses by STEM–EDS.

References

1. Allahverdi, M., Drew, R. A. L., Rudkowska, P., Rudkowski, G. and StromOlsen, J. O., Amorphous $CaO{\cdot}Al_2O_3$ fibers by melt extraction. *Mater. Sci. Eng. A—Struct. Mater. Prop. Microstruct. Process.*, 1996, **207**, 12–21.
2. Wallenberger, F. T., Brown, S. D. and Koutsky, J. A., Melt processing of optical alumina fibers—a process review and product outlook. *Sample Q.—Soc. Advance. Mater. Process Eng.*, 1992, **23**, 17–28.
3. Wallenberger, F. T., Weston, N. E. and Brown, S. D., Calcium aluminate glass-fibers—drawing from supercooled melts versus inviscid melt spinning. *Mater. Lett.*, 1991, **11**, 229–235.
4. Sakamoto, N., Watanabe, T. and Yoshimura, M., Fabrication of bulk glass from the eutectic melt in Y_2O_3–CaO–Al_2O_3 system. *J. Electroceram.*, 2006, **17**, 1075–1078.
5. Araki, S. and Yoshimura, M., Fabrication of transparent ceramics through melt solidification of near eutectic compositions in HfO_2–Al_2O_3–$GdAlO_3$ system. *J. Eur. Ceram. Soc.*, 2006, **26**, 3295–3299.
6. Sugiyama, A., Araki, S., Sakamoto, N., Watanabe, T. and Yoshimura, M., Fabrication of amorphous bulk and multi-phase ceramics by melting method in the HfO_2–Al_2O_3–Gd_2O_3–Eu_2O_3 system. *J. Electroceram.*, 2006, **17**, 71–74.
7. Hayashi, K., Matsuishi, S., Kamiya, T., Hirano, M. and Hosono, H., Light-induced conversion of an insulating refractory oxide into a persistent electronic conductor. *Nature*, 2002, **419**, 462–465.
8. Matsuishi, S., Toda, Y., Miyakawa, M., Hayashi, K., Kamiya, T., Hirano, M. *et al.*, High-density electron anions in a nanoporous single crystal: $[Ca_{24}Al_{28}O_{64}](4+)(4e(-))$. *Science*, 2003, **301**, 626–629.
9. Li, Q. X., Hayashi, K., Nishioka, M., Kashiwagi, H., Hirano, M., Torimoto, Y. *et al.*, Absolute emission current density of O^- from $12CaO{\cdot}7Al_2O_3$ crystal. *Appl. Phys. Lett.*, 2002, **80**, 4259–4261.
10. Kim, S. W., Miyakawa, M., Hayashi, K., Sakai, T., Hirano, M. and Hosono, H., Simple and efficient fabrication of room temperature stable electride: melt-solidification and glass ceramics. *J. Am. Chem. Soc.*, 2005, **127**, 1370–1371.
11. Sakamoto, N., Watanabe, T. and Yoshimura, M., Fabrication of crack-free C12A7 nano-ceramics composite from eutectic glass in the C12A7–$CaYAlO_4$ system. *Int. J. Appl. Ceram. Technol.*, 2006, **3**, 266–271.
12. Sung, Y. M. and Sung, J. H., Crystallization behaviour of calcium aluminate glass fibres. Part I. Differential thermal analysis study. *J. Mater. Sci.*, 1998, **33**, 4733–4737.
13. Mitchell, B. S., Yon, K.-Y., Dunn, S. A. and Koutsky, J. A., Phase identification in calcia–alumina fibers crystallized from amorphous precursors. *J. Non-Cryst. Solids*, 1993, **152**, 143–149.

14. Marquis, P. M., The crystallization of calcium aluminate glasses. *J. Microsc.*, 1981, **124**, 257–264.
15. Douy, A. and Gervais, M., Crystallization of amorphous precursors in the calcia–alumina system: a differential scanning calorimetry study. *J. Am. Ceram. Soc.*, 2000, **83**, 70–76.
16. Araki, S. and Yoshimura, M., Transparent nano-composites ceramics by annealing of amorphous phase in the HfO_2–Al_2O_3–$GdAlO_3$ system. *Int. J. Appl. Ceram. Technol.*, 2004, **1**, 155–160.
17. Jeevaratnam, J., Dent Glasser, L. S. and Glasser, F. P., Structure of calcium aluminate, $12CaO{\cdot}7Al_2O_3$. *Nature*, 1962, **194**, 764–765.
18. Hayashi, K., Hirano, M. and Hosono, H., Thermodynamics and kinetics of hydroxide ion formation in $12CaO{\cdot}7Al_2O_3$. *J. Phys. Chem. B*, 2005, **109**, 11900–11906.
19. Watauchi, S., Tanaka, I., Hayashi, K., Hirano, M. and Hosono, H., Crystal growth of $Ca_{12}Al_{14}O_{33}$ by the floating zone method. *J. Cryst. Growth*, 2002, **237**, 801–805.
20. Li, W. Y. and Mitchell, B. S., Nucleation and crystallization in calcium aluminate glasses. *J. Non-Cryst. Solids*, 1999, **255**, 199–207.